doi:10.2514/6.2022-2152
https://arc.aiaa.org/doi/abs/10.2514/6.2022-2152

Improving PIC-DSMC Simulations of Electrical Breakdown via Event Splitting

G. Oblapenko*
German Aerospace Center (DLR), 37073 Göttingen, Germany

D. Goldstein† and P. Varghese‡
The University of Texas at Austin, Austin, Texas, 78712

C. Moore§
Sandia National Laboratories, Albuquerque, New Mexico, 87185

A newly developed variable-weight DSMC collision scheme for inelastic collision events is applied to PIC-DSMC modelling of electrical breakdown in 1-dimensional helium and argon-filled gaps. Application of the collision scheme to various inelastic collisional and gas-surface interaction processes (electron-impact ionization, electronic excitation, secondary electron emission) is considered. The collision scheme is shown to improve the level of noise in the computed current density compared to the commonly used approach of sampling a single process, whilst maintaining a comparable level of computational cost and providing less variance in the average number of particles per cell.

I. Nomenclature

g	=	Magnitude of relative velocity of colliding particles
E	=	Electric field strength
j	=	Anode current density
$\hat{j}$	=	Prediced anode current density
N_p	=	Number of simulation particles
N_{proc}	=	Number of collision processes
N_{exc}	=	Number of excitation reactions
n	=	Number density
n_1, n_2	=	Computational particle weights
P_{el}	=	Elastic scattering probability
P_{exc}	=	Total electronic excitation probability
$P_{exc,i}$	=	Probability of electronic excitation to specific level i
P_i	=	Probability of process i
P_{ion}	=	Ionization probability
γ_{se}	=	Secondary emission probability
ω_{pe}	=	Plasma frequency
σ_i	=	Cross-section of process i
σ_{el}	=	Elastic scattering cross-section
σ_{exc}	=	Electronic excitation cross-section
σ_{ion}	=	Ionization cross-section

*Guest Postdoctoral Researcher, German Aerospace Center (DLR), Bunsenstraße 10, 37073 Göttingen, Germany
†Director of Computational Flow Physics Laboratory, Department of Aerospace Engineering and Engineering Mechanics, 2617 Wichita St., Stop C0600, AIAA Associate Fellow
‡Director of the Center for Aeromechanics Research, Department of Aerospace Engineering and Engineering Mechanics, 2617 Wichita St., Stop C0600, AIAA Associate Fellow
§Principal Member of Technical Staff, Plasma Theory & Simulation, Sandia National Laboratories, 87185-1168

II. Introduction

Numerical simulation of collisional plasmas is often performed using Particle-in-cell codes [1, 2] coupled with Direct Simulation Monte Carlo (DSMC) [3] collisions, also known as "PIC-DSMC" codes. The necessity of resolving extremely low populations, such as those of the high-velocity tails of the electron distribution function, trace chemical species (such as the charged particles) and excited electronic states, requires the use of variable-weight DSMC [4, 5]. Unlike "standard" DSMC, where each particle represents a single fixed number of real-life particles, in variable-weight DSMC, each particle can represent a different number of real-life particles. The variable-weight DSMC approach requires splitting of particles with differing computational weights during collisions, which complicates the algorithm due to the necessity of periodic particle merging [6, 7] in order to avoid exponential growth in the number of particles. However, in cases where multiple inelastic events can occur during a collision, the particle splitting can be leveraged: instead of choosing a single collision process (using acceptance-rejection) to be modelled, particles can be split further proportional to the probabilities of these processes, and all processes modelled simultaneously. We have previously shown that such an approach significantly reduces the level of stochastic noise in the computed ionization rate in an unsteady spatially homogeneous setup [8]. The resulting reduction in stochastic noise may be beneficial to unsteady PIC-DSMC simulations such as streamer propagation [9, 10], as low-probability events can significantly affect the flow physics, perhaps even qualitatively. Due to the unsteady nature of such problems, reducing stochastic noise levels requires either the use of a larger number of computational particles, or ensemble averaging over multiple simulations — approaches which may not always be viable due to computational time and/or machine memory constraints.

In the present work, the event splitting approach is expanded to account for is electronic excitation processes and is applied to a fully coupled PIC-DSMC simulation of breakdown in a 1-dimensional gap.

III. Event Splitting in Variable Weight DSMC

In variable-weight DSMC, when two particles with computational weights n_1 and n_2 collide, the particle with the larger computational weight (which, without loss of generality, we assume to have weight n_1) is split into two particles: one with weight $n_1 - n_2$ and another with weight n_2. The two particles with equal weights n_2 are then collided, whilst the particle with weight $n_1 - n_2$ retains its velocity. In case multiple processes can occur during the collision (for example, during an electron-neutral atom collision, possible processes include elastic scattering, ionization, and electronic excitation), the specific process to be simulated is chosen based on its probability $P_i(g)$, where $P_i(g) = \sigma_i(g)/\sum_i \sigma_i(g)$. Here $\sigma_i(g)$ is the cross-section of the corresponding process, and g is the magnitude of the relative velocity of the colliding particles. Thus, in case of processes with low-probability, it can be expected that they will be selected less frequently, which will lead to a higher level of stochastic noise in the distributions of the post-collision particles resulting from the rare collision event.

Figure 1 shows an example of the standard DSMC collision procedure in a variable-weight framework (for an argon-electron collision with two possible outcomes: elastic collision or ionization): firstly, after particles are chosen for collision (in this work, we use the variable-weight selection procedures developed in [11], which generalize the NTC scheme [3] to variable-weight particles), the particle with the larger computational weight is split, and then a specific process type is sampled and simulated (the probabilities of the specific processes are shown next to the arrows leading from the sampling step).

Our proposed algorithm, which we will refer to as "event splitting" [8, 12], consists of the following steps: an additional particle split is performed for the two equal-weight particles based on the probabilities of the possible collision events that can occur for the considered collision. After the initial split step (during which the particle with the larger computational weight is split into two smaller particles) the (equal weight) particles are split further into N_{proc} smaller particles, with weights $n_2 P_i,\ i = 1, \ldots, N_{proc}$, where $P_i(g) = \sigma_i(g)/\sum_i \sigma_i(g)$. Here N_{proc} is the number of possible collision processes. After this second split, all the possible collision outcomes are simulated (instead of a single collision process being simulated for each collision pair in a given timestep). The aim of the approach is to reduce variance in the simulation of inelastic processes, especially those with low probabilities and increase the accuracy of modelling where these low-probability processes can have a significant impact on the flow physics.

Figure 2 shows the same set of processes modelled as Fig. 1 using the proposed event splitting scheme: the initial splitting step is retained, but no sampling step is performed, and all collision outcomes (in this case, 2) are simulated simultaneously. Thus, more particles are produced (in the shown case, 6 particles), but with smaller computational weights.

This algorithm may also be applied for boundary conditions: for example, in the case of secondary emission of electrons from a cathode, instead of emitting an electron with computational weight n_1 with a probability of γ_{se} each

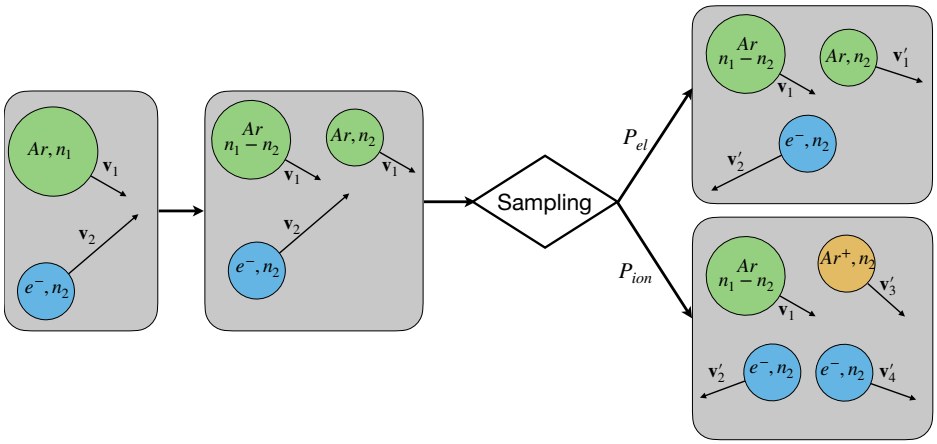

Fig. 1 Example of standard collision procedures in variable weight DSMC. Velocities of the particles are denoted by the vectors $\mathbf{v}_i$, new post-collision velocities are denoted by the primed vectors $\mathbf{v}'_i$. The computational weights of the particles are denoted by the quantities n_i. The arrows with the probabilities (P_{el}, P_{ion}) next to the sampling step show the possible sampled events, along with their corresponding probabilities.

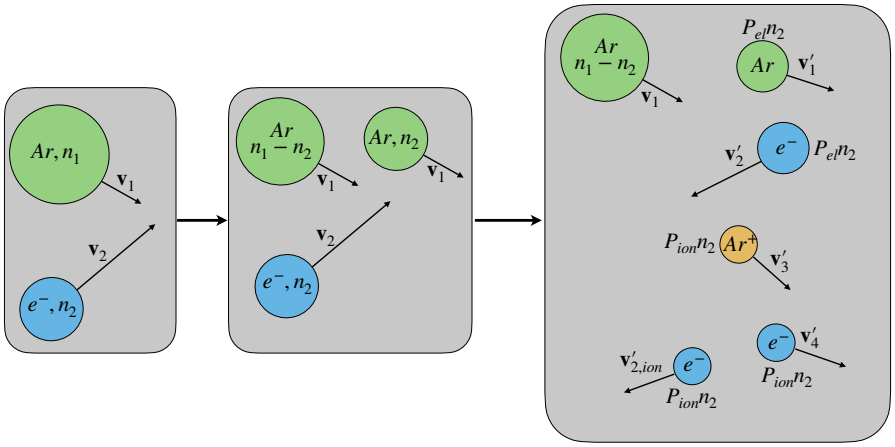

Fig. 2 Example of collision procedures in variable weight DSMC using the proposed event splitting scheme.

time an ion with computational weight n_1 strikes the cathode, an electron with computational weight $\gamma_{se} n_1$ can be emitted for each ion with computational weight n_1 striking the cathode.

Figures 3–4 show a schematic of the treatment of secondary emission at the cathode using the standard DSMC approach and the event splitting procedure, respectively. Naturally, the reduction in variance of the simulation of secondary emission when using event splitting directly depends on the specific value of the secondary emission coefficient γ_{se}.

In the present work we consider ionized argon flows and perform simulations with and without electron-impact electronic excitation. Thus, the modelled processes always include electron-neutral elastic scattering and electron-impact ionization, as well as elastic collisions of the background neutral gas. In case electron-impact excitation reactions are included in the simulation, we consider them only as an energy sink: the excited states are not modelled, only the loss of energy of the impacting electron is simulated. The cross-sections are taken from the BSR data [13, 14], and the Okhrimovskyy model [15] is used to simulate the electron scattering.

Figure 5 shows the elastic, electronic excitation and ionization cross-sections. It can be seen that already at a

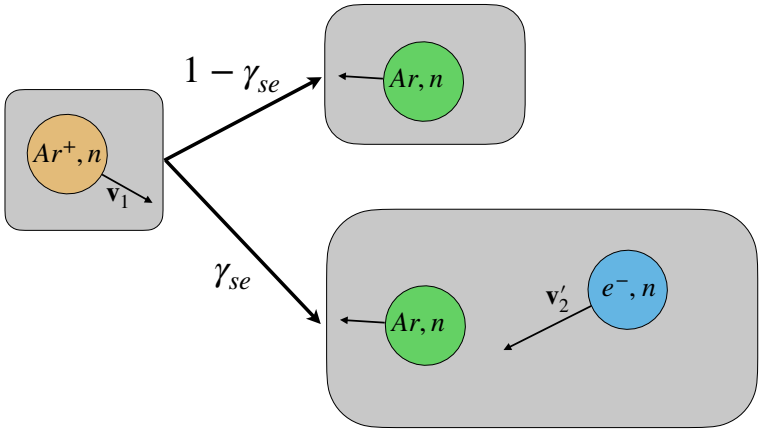

Fig. 3 Standard DSMC procedure for modelling secondary emission from cathode.

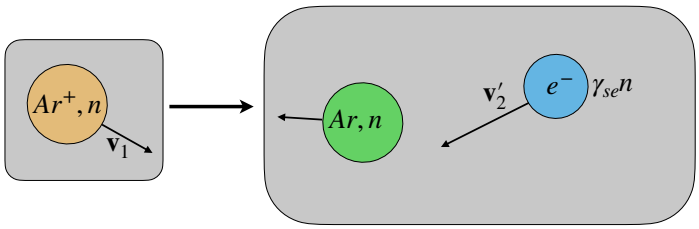

Fig. 4 Proposed event splitting DSMC procedure for modelling secondary emission from cathode.

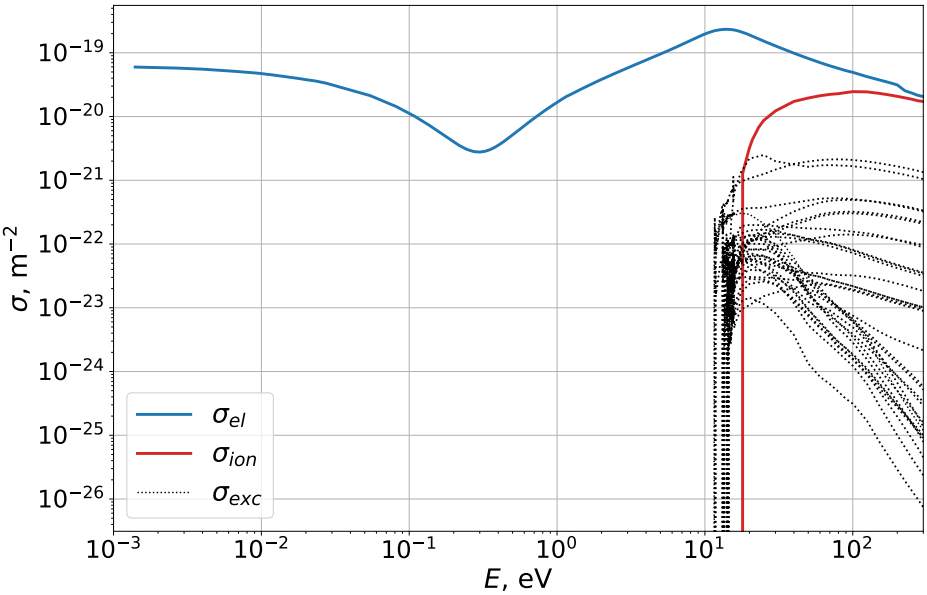

Fig. 5 Electron-impact cross-sections for argon atoms.

translational energy of approximately 30 eV, the probability of an ionization reaction is around 10%, and it continues to increase with increasing translational energies (as the elastic cross-section rapidly decreases above energies of 10 eV). The excitation cross-sections, on the other hand, are significantly smaller, and as a consequence, the probabilities of these processes are minuscule compared to the ionization and elastic cross-sections. However, accurate simulation of these excitation processes is needed not only to account for the energy loss of the electrons in the flow, but also to model

the photon emission from the excited states, which may be a significant sources of electrons at the cathode [10, 16].

IV. Numerical Results

The simulations were performed using an in-house variable weight DSMC solver. The octree-based merging algorithm [7] was used to control the particle count. Merging was performed species-wise: when the number of particles of a particular in a cell exceeded 110% of the target particle number for the particular species, merging was performed (with the resulting post-merge number of particles being approximately equal to the target particle number).

The 1-dimensional simulations were performed using a fully coupled PIC-DSMC algorithm. Velocity Verlet integration was used for the particle convection and acceleration, and the tridiagonal matrix algorithm was used for the Poisson equation solver. The secondary emission coefficient was taken to be 0.1.

A. 0-D Ionization Simulation

We first consider a simple spatially homogenous test case in order to verify the validity of the event splitting approach, as well as compare the performance of the scheme in terms of noise and computational speed to the usual variable-weight NTC scheme. The event splitting approach was used to simulate electron-impact ionization in a spatially homogenous argon-electron mixture accelerated by a constant electric field (with a reduced field strength of 50 Td). The computed electron density was used to obtain the instantaneous electron-impact ionization rate coefficient, for which statistics were gathered over 600,000 timesteps. The target number of particles in the simulation was varied from 200 to 60000 (since a variable-weight DSMC algorithm is used throughout the paper, the number of particles varies due to occasional particle merging).

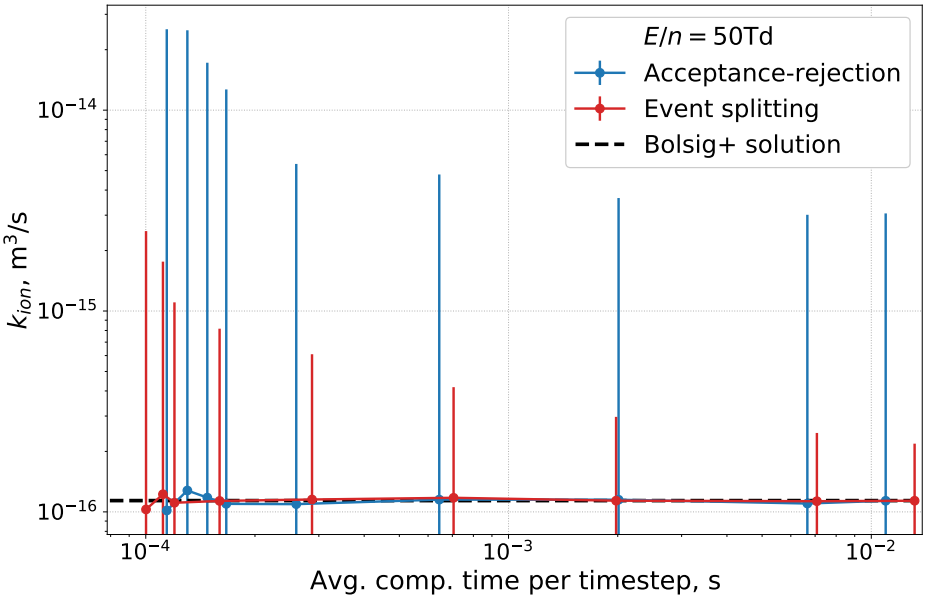

Fig. 6 Computed ionization rate coefficient plotted against average time per collision step.

Figure 6 shows the computed electron-impact ionization rate coefficient plotted against the average computational time per collision step. The reference solution produced by the Bolsig+ solver [17] is shown by the black dashed line. The vertical bars denote a range of one standard deviation. As the number of computational particles is increased, the computational cost rises as well, and the level of stochastic noise decreases. It can be seen that the use of the event splitting scheme leads to a much lower level of stochastic noise in the ionization rate coefficient, and that the cost of the simulations performed using event splitting is not much higher than that of the simulations performed using acceptance-rejection.

Figure 7 shows the relative error in the ionization rate coefficient as a function of the average number of simulation particles (since a variable-weight DSMC algorithm is used, the number of particles varies from timestep to timestep due to particle splitting and merging). It can be seen that the error in the ionization rate coefficient scales linearly with

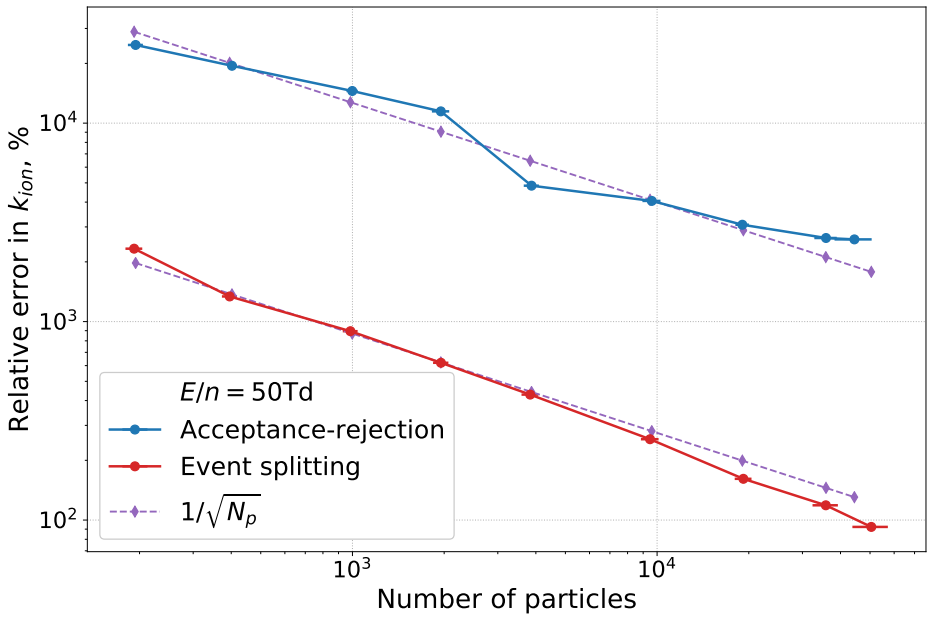

Fig. 7 Relative error in the computed ionization rate coefficient plotted against average number of simulation particles.

$1/\sqrt{N_p}$ for both the acceptance-rejection and event splitting schemes, but is significantly lower when event splitting is used.

B. 1-D Breakdown Simulation Without Electronic Excitation

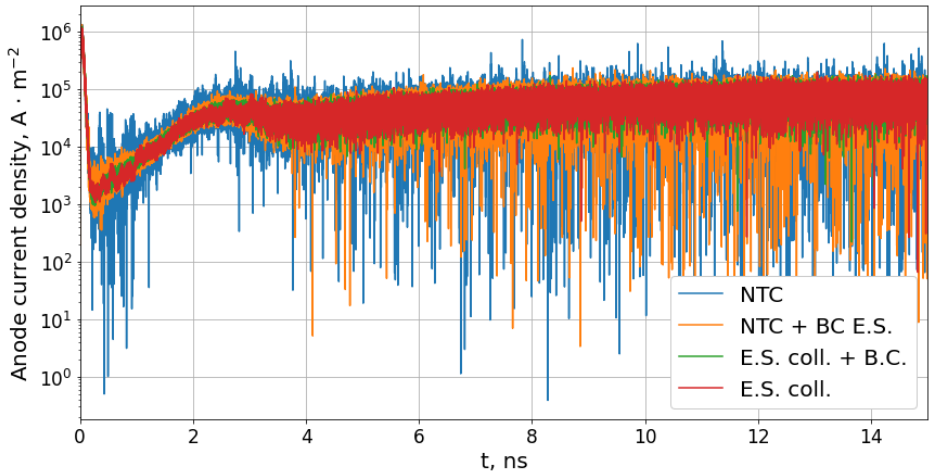

Fig. 8 Anode current density as a function of time.

Next, we consider the process of a 1-dimension electrical breakdown simulation in a narrow gap. The gap width was taken to be 50 μm, and the background gas pressure was taken to be 100 Torr. The voltage drop across the gap was set to 200 V, and the secondary emission coefficient γ_{se} was assumed to be 0.1 (an electron is emitted with a probability of 10% each time an ion hits the cathode). 150 uniformly-sized cells were used to discretize the domain, and the average number of particles per cell was varied from 150 particles/cell to 2000 particles/cell. A timestep of 5.18×10^{-15} s was used. At the start of the simulation, the mean time between electron-neutral collisions is approximately 5.4×10^{-13} s, the plasma frequency ω_{pe} is $5.6{\times}10^{10}$ s^{-1} (corresponding to a plasma oscillation timescale of 1.78×10^{-11} s), and the

Debye length is 1.2 μm.

Figure 8 shows the anode current density as a function of time. The "NTC" curve shows the anode current density obtained using a "standard" DSMC approach, with a single collision process simulated for each electron-impact collision, and an acceptance-rejection scheme for the secondary emission. The "NTC + BC E.S." curve uses the event splitting for the boundary condition treatment (each ion hitting the cathode results in an electron being emitted with a computational weight equal to 0.1 of the ion's computational weight), but keeps the "standard" DSMC approach for electron-neutral collisions. It can be seen that all simulations lead to an exponential rise in anode current density, and that the use of event splitting reduces the noise in computed current density, especially if event splitting is used for argon-electron collisions ("E.S. coll." and "E.S. coll. + B.C." curves). The use of event splitting for collisions also helps to maintain sufficiently high particle counts in all cells, whereas the simulations using acceptance-rejection for neutral-electron collisions suffer from insufficient particle counts, and require the use of particle cloning [7] in order to provide correct results. Moreover, the particle cloning routine does not introduce new information into the system, and the fidelity of the simulation is improved only through the subsequent collisions of the cloned particles, whilst the use of event splitting allows one to avoid the cloning procedure and maintain sufficient particle counts through a physically meaningful approach.

In order to quantify the noise in the simulation, we consider the following metric. We assume that the anode current density j grows exponentially after 8 ns. We fit a linear regression model to the quantity $\log j$, and for each simulation, compute the Root Mean Squared Log Error (RMSLE) relative to the regression model fitted to the anode current density obtained with that specific simulation:

$$RMSLE = \sqrt{\frac{1}{n_t} \sum_{t>8\ ns} \left(\log j(t) - \log \hat{j}(t)\right)^2}. \tag{1}$$

Here n_t is the number of timesteps over which the metric is computed, and $\hat{j}(t)$ is the anode current density at time t as predicted by the linear regression model.

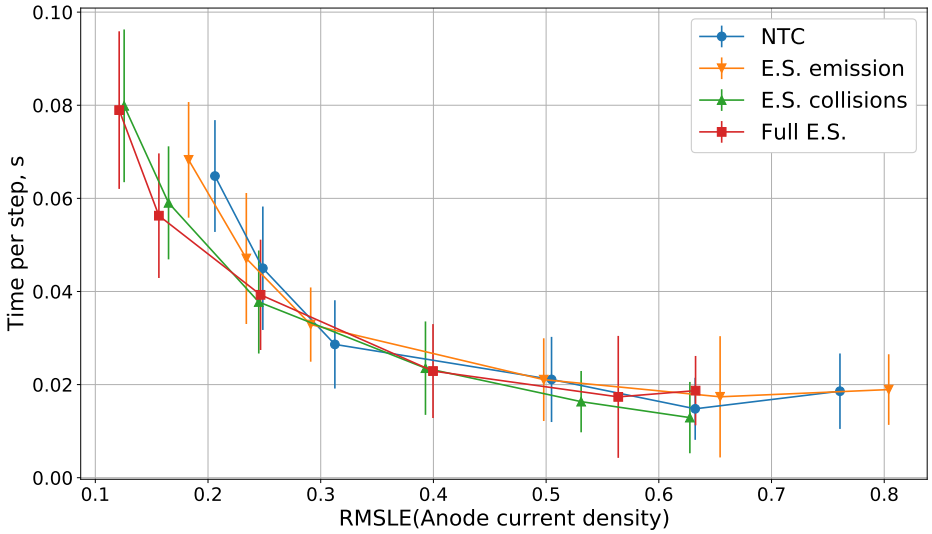

Fig. 9 Computational time per timestep plotted against the noise in the anode current density.

Figure 9 shows the average computational time per timestep plotted against the noise in the anode current density. The vertical error bars denote a range of one standard deviation. It can be seen that when event splitting is used for collisions ("E.S. collisions" and "Full E.S." curves), the performance-to-noise ratio is somewhat improved compared to the standard DSMC simulation ("NTC" curve) and the simulation that used event splitting only for secondary emission ("E.S. emission"). The improved performance of the event splitting scheme in terms of variance reduction is somewhat offset by the higher computational cost (as all possible collision outcomes need to be simulated, which requires computation of multiple scatterings). It should be noted that the relative performance of the different collision and boundary condition treatment schemes depends strongly on the cross-sections used, the voltage applied, and the secondary emission coefficient value. Thus, under different conditions (e.g., a lower secondary emission coefficient), the benefits of the event splitting scheme might be more evident.

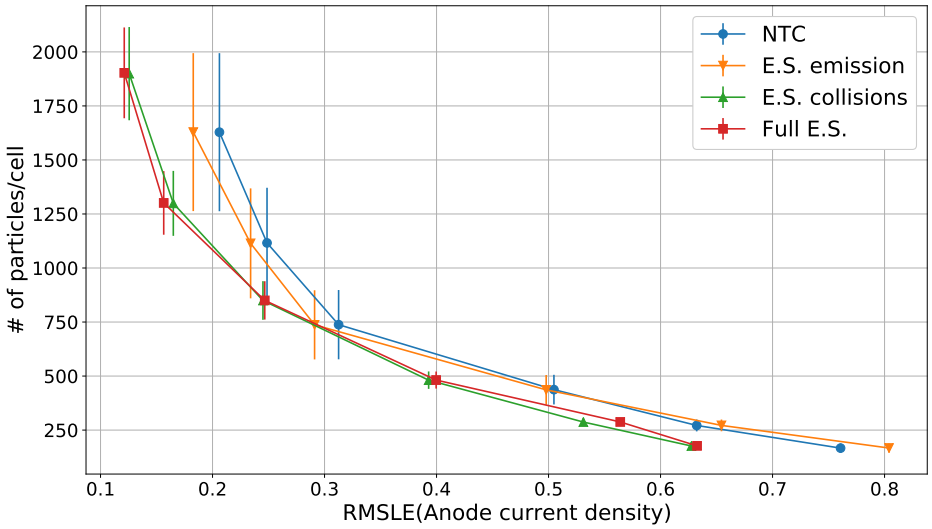

Fig. 10 Number of computational particles per cell plotted against the noise in the anode current density.

We also look at the relationship between the average number of particles per cell and noise in the anode current density, as shown on Fig. 10. Here, the benefits of using the event splitting scheme are seen more clearly. For a given level of noise, one needs fewer particles per cell (up to 30%) to achieve the same level of accuracy as compared to standard DSMC. Or, for a given average number of particles per cell, the level of noise in the simulation is reduced. This is important for modern large scale computations, as simulations are often memory-bound, especially when Graphical Processing Units (GPUs) are utilized. The reduction in the variance of the number of particles per cell when event splitting is used for collisions is also noteworthy. Again, such an improvement in the memory usage consistency is important for GPU-based simulations, as it allows for less thread divergence when threading over elements.

Thus, for the considered case of a fully coupled PIC-DSMC simulation of breakdown in an argon-filled gap with two possible neutral-electron collision processes, the event splitting scheme provides some benefits in terms of stochastic noise level for a given level of computational effort, and more significant benefits in terms of stochastic noise level for a given number of simulation particles per cell.

C. 1-D Breakdown Simulation With Electronic Excitation

Next, we include the 31 electron-impact electronic excitation cross-sections into consideration. At least two options are possible: 1) one can perform event splitting based on *collision processes type*, or 2) one can perform event splitting based on *collision processes*. By the first approach we understand that for every electron-neutral collision with sufficient translational energy, a 3-way split is performed (proportionally to the probabilities of elastic scattering, ionization, and the total probability of an excitation reaction), and the specific excitation reaction to be simulated is chosen using the standard DSMC sampling approach. So for each collision pair, no more than one excitation reaction is performed. Within the second approach, all the possible excitation reactions are simulated for each collision. Naturally, the first approach can be based on grouping the collision processes not by process type, but by some other criteria, such as probability or threshold energy.

Figure 11 shows a schematic of the event splitting based on collision processes in an argon gas with electron-impact electronic excitation, ionization, and elastic scattering of electrons. The inner bounding box and the period sign inside denote that not all the products of the electronic excitation reaction are shown. It is evident from the schematic that a very large number of particles are produced: for 31 excitation reactions, $2 \times 31 + 3 + 3 = 68$ particles are produced from the initial 2 particles for a sufficiently high-energy collision, of which 34 are electron particles. One might anticipate that this will lead to very frequent merging, and as a result, a significant distortion of the electron velocity distribution function, which may prove to have a significant detrimental influence on the flow.

Figure 12 shows a schematic of the event splitting algorithm based on the process type (the initial particle splitting step is not shown explicitly). Sampling is performed to choose which specific excitation reaction to simulate. From the initial 2 particles a total of 8 particles are produced (3 neutral particles, 1 ion, and 4 electron particles).

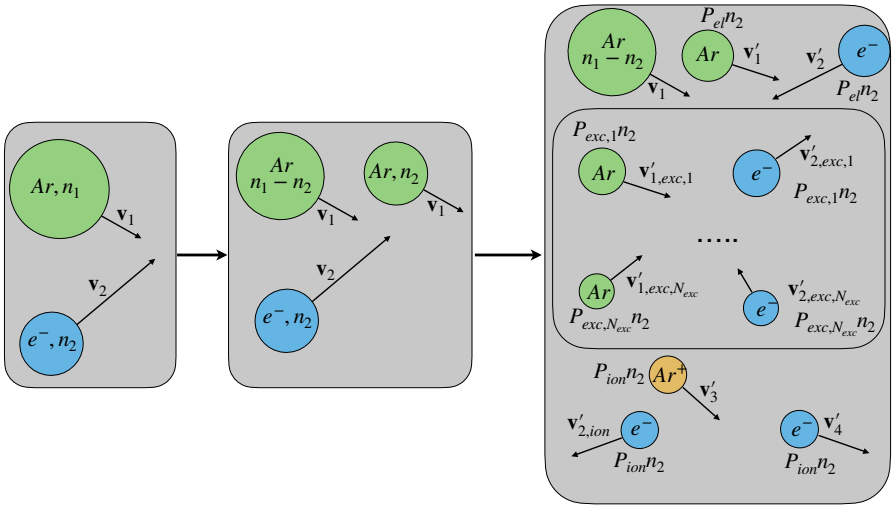

Fig. 11 Schematic of event splitting algorithm based on collision processes.

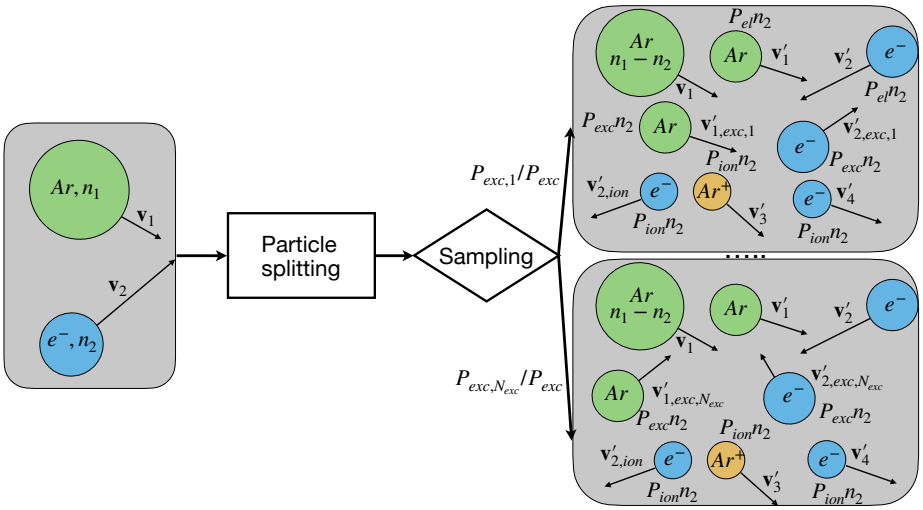

Fig. 12 Schematic of event splitting algorithm based on process type.

In order to compare the two different collision event splitting approaches, we performed a 0-D simulation of an ionized gas accelerated by a constant electric field and computed the time-averaged ionization rate coefficient. The target particle number was set to 2000 particles for each species.

Figure 13 shows the evolution of the ion number density as a function of time. It is immediately evident that when event splitting is performed based on collision processes, and not process types ("Full event splitting" curve), the ionization rate is much higher than when either no event splitting is performed, or when event splitting is performed based on process type. In order to investigate the cause of this discrepancy, we performed simulations using reduced excitation reaction sets, and compared the computed ionization rate coefficient to that obtained with Bolsig+ on the same reduced reaction set.

Figure 14 shows the error in the ionization rate coefficient relative to the Bolsig+ solver (solid lines) and average number of timesteps between merging events (dashed lines) as a function of the number of excitation reactions considered. When event splitting is performed based on process type (blue lines), the error stays relatively constant, as well as the average number of timesteps between particle merges. As the number of excitation reactions included in the reaction set does not influence the fact that at most 1 excitation event is simulated for a collision pair, the post-collision number of particles is not influenced by the number of excitation reactions considered, and the rate of growth of the particle number stays constant. In contrast, when full event splitting is used (red lines), the more reactions that are included in

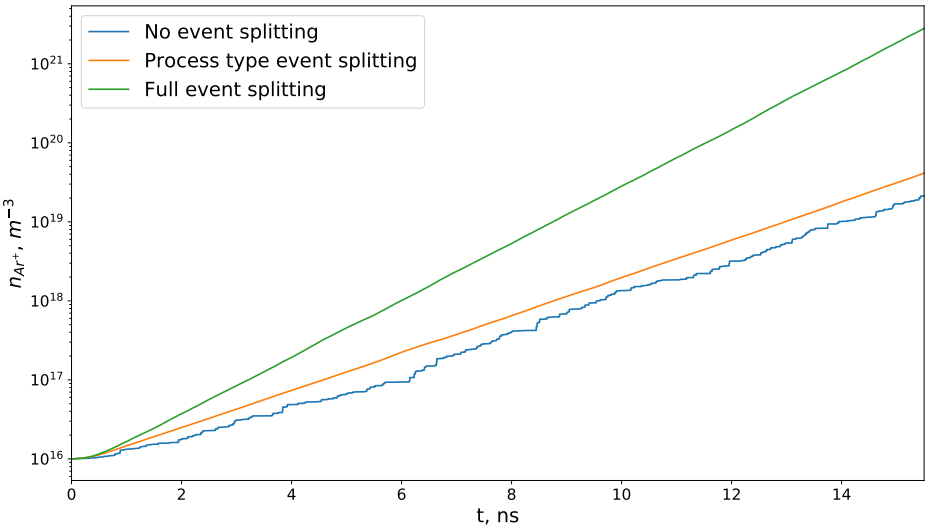

Fig. 13 Ion number density as a function of time.

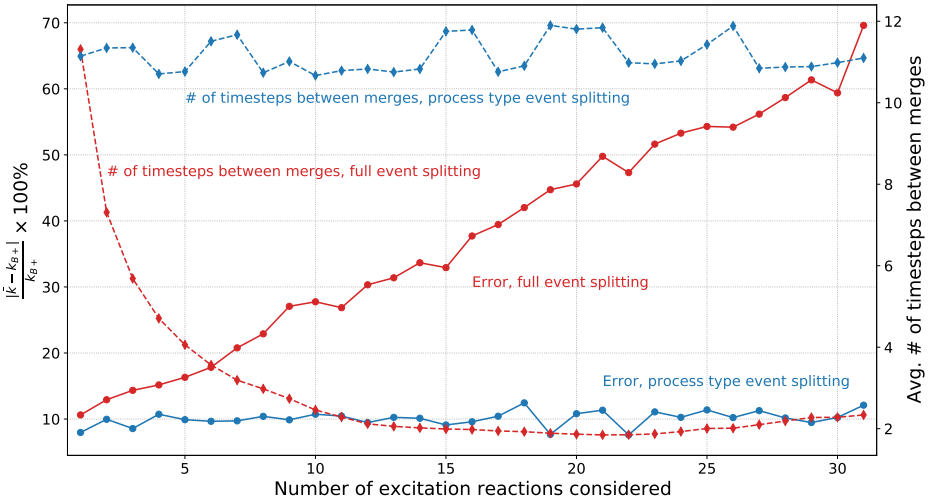

Fig. 14 Error in the ionization rate coefficient relative to the Bolsig+ solver (solid lines) and average number of timesteps between merging events (dashed lines) as a function of the number of excitation reactions considered. Red lines correspond to full event splitting, blue lines correspond to process type event splitting.

the reaction set, the more particles are produced during sufficiently energetic collisions. As a consequence, merging has to be performed more and more often, and it is this frequent merging which distorts the distribution function strongly enough so as to cause a strong deviation in the computed ionization rate coefficient from the expected value. Thus, one has to consider the balance between the potential benefit of event splitting and the errors introduced by more frequent merging.

As a result of this simplified analysis, in the 1-D simulations with electronic excitation reactions presented below, we only perform event splitting based on the process type. In the 1-D simulations presented below, the average number of particles per cell was varied from 150 particles/cell to 900 particles/cell. The other parameters (number of cells, gap width, pressure, timestep, voltage drop) were taken to be identical to those used in the 1-D simulations without electronic excitation.

Figure 15 shows the anode current density as a function of time. One can notice that simulations that use event splitting for the electron-neutral collision process ("E.S. coll", "E.S. coll. + B.C.") produce a somewhat slower growth of the anode current density. One possible explanation for such a discrepancy is the following: the electronic excitation

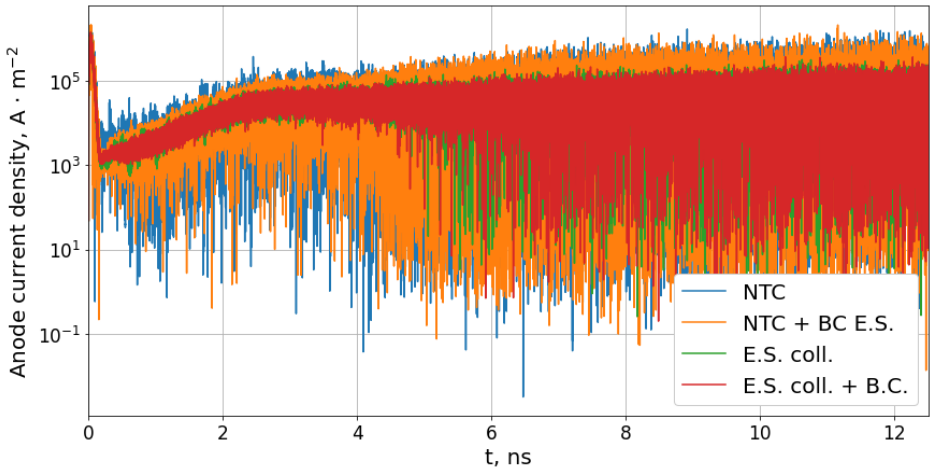

Fig. 15 Anode current density as a function of time.

events have a very low probability (as can be seen from Fig. 5). Thus, when the standard NTC collision algorithm is used, these events are simulated very rarely. When event splitting is used, all sufficiently energetic collisions between argon neutrals and electrons lead to a loss of the electron energy, and thus, the anode current density grows at a slower rate, as the ionization rate is attenuated due to the electronic excitation "energy sink". If the very low probability of sampling an electronic excitation reaction is indeed the cause of the discrepancy, when using the standard NTC routine, one would either have to a) perform ensemble averaging when using the standard NTC collision routine or b) use a sufficiently high number of particles to avoid the issue. However, a further investigation of the causes of the discrepancy between the different routines is necessary to obtain conclusive results.

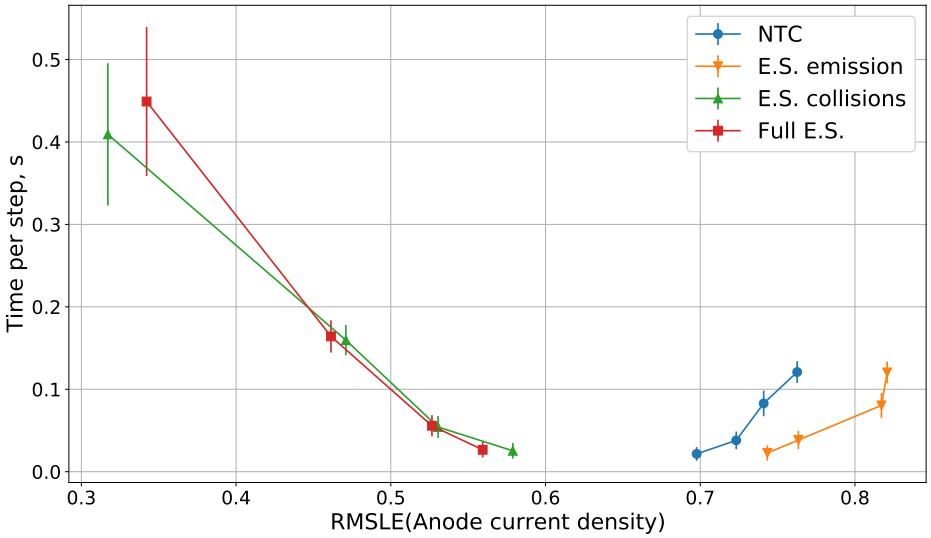

Fig. 16 Computational time per timestep plotted against the noise in the anode current density.

As for the case without electronic excitation, we look at the computational cost-vs-noise metric to compare the different collision and boundary condition algorithms. Figures 16–17 show the average computational time per timestep and average number of computational particles per cell plotted against the noise (as measured by the RMSLE metric) in the anode current density, respectively. Surprisingly, when one does not use the event splitting scheme for collisions, the increasing the number of particles (and as a consequence, the computational time per timestep) in the simulation leads to increased noise in the anode current density. This is possibly due to the issue mentioned earlier, of electronic excitation events being rarely sampled due to their low probability. If one increases the number of particles per cell, the number of

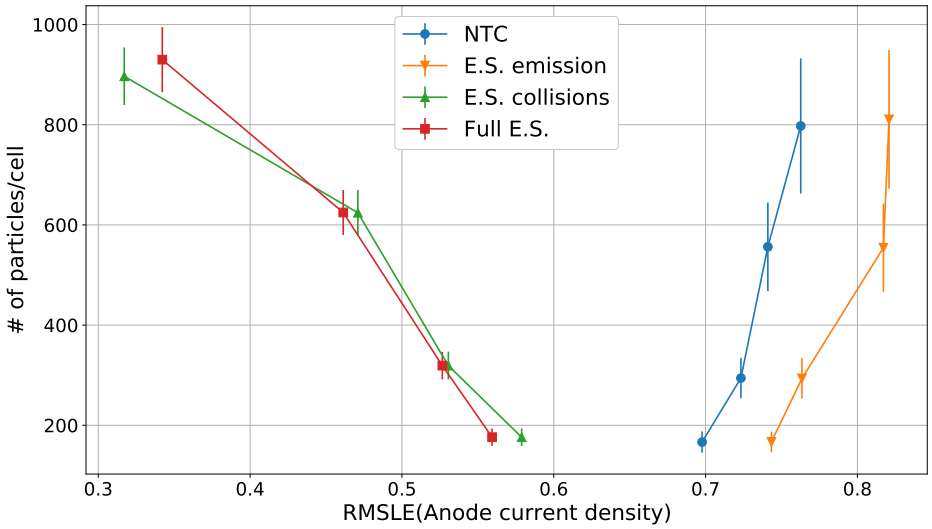

Fig. 17 Number of computational particles per cell plotted against the noise in the anode current density.

collisions each timestep is also increased. As a consequence, electronic excitation events are sampled more frequently, and the distribution function is sufficiently changed due to the improved sampling of electronic excitation events, which shows up as an increased level of noise in the simulation (since each event removes a significant amount of the electron's energy). Then one would expect that with sufficient ensemble averaging or with higher particle counts, the noise would start to be inversely correlated with the number of particles. If this excitation reaction sampling issue is indeed the cause for such results, that points to another benefit of the event splitting scheme, as then one can avoid having to use very high particle counts or perform ensemble averaging in unsteady simulations with low-probability events.

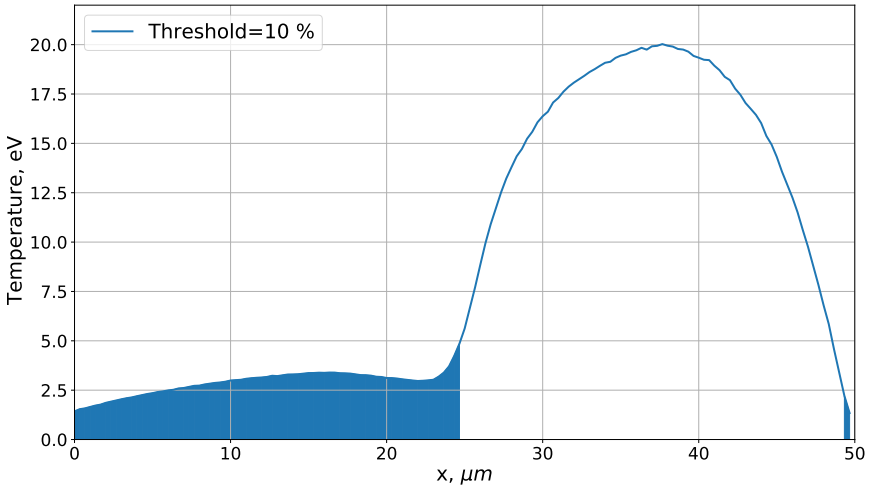

Fig. 18 Time-averaged electron temperature plotted across the simulation domain, with the filled-in blue part showing areas of the domain where hybridization might be applied

Finally, we also consider the potential avenues for velocity-space hybridization [18, 19] of variable-weight DSMC with a discrete velocity-based Boltzmann solver. One of the benefits of discrete velocity-based solvers is their ability to accurately resolve the tails of the velocity distribution function. A velocity-space hybridization with DSMC is performed by using DSMC particles to represent the bulk of the distribution function and using a discrete velocity representation to model the high-speed tails of the distribution. Such an approach provides a computational speed-up over a pure discrete velocity-based solver, and allows one to achieve a lower level of noise compared to DSMC. Previous work on velocity space hybridization as applied to ionized flow simulation showed that the species that benefit the most from

such a hybrid representation are the electrons (since it is the high-velocity electrons that drive ionization and excitation processes). Thus, in a 1-D breakdown simulation, one would be interested in using such a hybrid approach in certain areas of the domain, namely, where the electron distribution is cold, and accurately capturing the tails of the electron distribution function may be complicated even with variable-weight, event splitting DSMC method.

In order to assess in which areas of the domain such a hybrid approach might be used, we used time averaged binned distributions obtained from the simulation that used 900 particles per cell and event splitting both for collisions and secondary emission. Based on these time averaged distributions, we assume that cells in the spatial domain where less than 10% of the electrons have an energy sufficient enough to cause an ionization reaction would benefit from a velocity space hybridization.

Figure 18 shows the time-averaged electron temperature plotted across the domain, with the area below the curve filled in in those regions of the domain where less than 10% of the electrons have an energy sufficient enough to cause an ionization reaction. It can be seen that a significant portion of the domain might benefit from the application of a velocity space hybridization; although the exact area of application might also depend on the quantity of interest being studied. It should also be noted that the variation of the electron temperature is relatively small in the filled-in region, and one might potentially avoid having to use adaptive velocity space grids, as no drastic changes in the velocity distribution function need to be accommodated.

V. Conclusion

The event splitting approach for variable-weight DSMC simulations has been expanded to include electronic excitation reactions (within a simplified approach, in which such reactions act only as an electron energy sink). PIC-DSMC simulations of breakdown in an argon-filled gap *without* accounting for electronic excitation reactions show that the event splitting scheme provides some benefits in terms of level of noise in the anode current density for a given average number of particles per cell, especially when used for the collision process (and not only the boundary conditions). Simulations performed *with* electronic excitation included show that the event splitting scheme should be applied with care to processes with multiple collision outcomes in order to avoid over-aggressive merging (and the ensuing error in the velocity distribution function and inelastic process rates). Breakdown simulations performed accounting for electronic excitation show that event splitting when applied to collisions reduces the level of noise significantly (compared to the NTC collision scheme). The unexpected behaviour of the NTC collision scheme in this case requires a more thorough investigation. The potential area of application of a velocity space hybridization-based simulation approach is also considered based on results obtained with DSMC.

Acknowledgments

This work was supported by Sandia National Laboratories. Sandia National Laboratories is a multimission laboratory managed and operated by National Technology and Engineering Solutions of Sandia, LLC., a wholly owned subsidiary of Honeywell International, Inc., for the U.S. Department of Energy's National Nuclear Security Administration under contract DE-NA0003525. This paper describes objective technical results and analysis. Any subjective views or opinions that might be expressed in the paper do not necessarily represent the views of the U.S. Department of Energy or the United States Government. SAND2021-14694C

Georgii Oblapenko acknowledges the funding provided by the Alexander von Humboldt foundation for his stay as a guest researcher at the German Aerospace Center (DLR).

References

[1] Birdsall, C. K., "Particle-in-cell charged-particle simulations, plus Monte Carlo collisions with neutral atoms, PIC-MCC," *IEEE Trans. Plasma Sci.*, Vol. 19, No. 2, 1991, pp. 65–85.

[2] Serikov, V. V., Kawamoto, S., and Nanbu, K., "Particle-in-cell plus direct simulation Monte Carlo (PIC-DSMC) approach for self-consistent plasma-gas simulations," *IEEE Trans. Plasma Sci.*, Vol. 27, No. 5, 1999, pp. 1389–1398.

[3] Bird, G. A., *Molecular Gas Dynamics and the Direct Simulation of Gas Flows*, Clarendon, Oxford, England, UK, 1994.

[4] Rjasanow, S., and Wagner, W., "A stochastic weighted particle method for the Boltzmann equation," *J. Comput. Phys.*, Vol. 124, No. 2, 1996, pp. 243–253.

[5] Araki, S., and Martin, R., "Interspecies fractional collisions," *Phys. Plasmas*, Vol. 27, No. 3, 2020, p. 033504.

[6] Boyd, I. D., "Conservative species weighting scheme for the direct simulation Monte Carlo method," *J. Thermophys. Heat Transfer*, Vol. 10, No. 4, 1996, pp. 579–585.

[7] Martin, R. S., and Cambier, J.-L., "Octree particle management for DSMC and PIC simulations," *J. Comput. Phys.*, Vol. 327, 2016, pp. 943–966.

[8] Oblapenko, G., Goldstein, D. B., Varghese, P., and Moore, C., "Modeling of Ionized Gas Flows with a Velocity-space Hybrid Boltzmann Solver," *AIAA Scitech 2021 Forum*, 2021, p. 0705.

[9] Fierro, A., Moore, C., Yee, B., and Hopkins, M., "Three-dimensional kinetic modeling of streamer propagation in a nitrogen/helium gas mixture," *Plasma Sources Sci. Technol.*, Vol. 27, No. 10, 2018, p. 105008.

[10] Lietz, A. M., Barnat, E. V., Nail, G. R., Roberds, N. A., Fierro, A. S., Yee, B. T., Moore, C. H., Clem, P., and Hopkins, M., "High-Fidelity Modeling of Breakdown in Helium: Initiation Processes and Secondary Electron Emission," *Journal of Physics D: Applied Physics*, 2021.

[11] Schmidt, D. P., and Rutland, C., "A new droplet collision algorithm," *J. Comput. Phys.*, Vol. 164, No. 1, 2000, pp. 62–80.

[12] Oblapenko, G., Goldstein, D. B., Varghese, P., and Moore, C., "Hedging Direct Simulation Monte Carlo Bets via Event Splitting," *submitted to J. Comput. Phys.*, 2021.

[13] Pitchford, L., Alves, L., Bartschat, K., Biagi, S., Bordage, M., Phelps, A., Ferreira, C., Hagelaar, G., Morgan, W., Pancheshnyi, S., et al., "Comparisons of sets of electron–neutral scattering cross sections and swarm parameters in noble gases: I. Argon," *J. Phys. D: Appl. Phys.*, Vol. 46, No. 33, 2013, p. 334001.

[14] Zatsarinny, O., Wang, Y., and Bartschat, K., "Electron-impact excitation of argon at intermediate energies," *Phys. Rev. A*, Vol. 89, No. 2, 2014, p. 022706.

[15] Okhrimovskyy, A., Bogaerts, A., and Gijbels, R., "Electron anisotropic scattering in gases: A formula for Monte Carlo simulations," *Phys. Rev. E*, Vol. 65, No. 3, 2002, p. 037402.

[16] Fierro, A., Moore, C., Scheiner, B., Yee, B. T., and Hopkins, M. M., "Radiation transport in kinetic simulations and the influence of photoemission on electron current in self-sustaining discharges," *J. Phys. D: Appl. Phys.*, Vol. 50, No. 6, 2017, p. 065202.

[17] Hagelaar, G., and Pitchford, L., "Solving the Boltzmann equation to obtain electron transport coefficients and rate coefficients for fluid models," *Plasma Sources Sci. Technol.*, Vol. 14, No. 4, 2005, p. 722.

[18] Oblapenko, G., Goldstein, D. B., Varghese, P., and Moore, C., "A velocity space hybridization-based Boltzmann equation solver," *J. Comput. Phys.*, Vol. 408, 2020, p. 109302.

[19] Oblapenko, G., Goldstein, D. B., Varghese, P., and Moore, C., "Velocity-Space Hybridization of Direct Simulation Monte Carlo and a Quasi-Particle Boltzmann Solver," *Journal of Thermophysics and Heat Transfer*, Vol. 35, No. 4, 2021, pp. 788–799.